and 8% and recording the change in ICBF after a 2–3 min stabilization period. These paired values of $ETCO_2$ and ICBF were then used to calculate the regression equation of ICBF on $ETCO_2$, the coefficient of which represented the quantitative expression of $CO_2R$ ($\Delta$ %ICBF/$\Delta$ %$ETCO_2$). Second, MAP was varied above and below the resting level and $CO_2R$ determinations were then repeated for each MAP level and used to calculate the slopes and intercepts of the regression of $CO_2R$ on MAP for the particular animal. These values were then averaged within each experimental group to yield the mean slopes and intercepts shown in the table. Four to six steps of MAP, over the range of 45–105 mm Hg, were studied in each animal. Results were assessed by analysis of variance and LSD test[6].

*Results.* Average $CO_2R$ prior to interventions designed to modify MAP was 14 ± 1.5 (SE) ($\Delta$ %ICBF/$\Delta$ % $ETCO_2$). Average MAP was 78 ± 2.3 mm Hg.

Reduction in MAP by bleeding led to a progressive increase in $CO_2R$ while increase in MAP by infusion of phenylephrine produced a corresponding reduction of $CO_2R$ (table, A). Equivalent increase in MAP produced by aortic occlusion was accompanied by the same reduction in $CO_2R$ as observed with infusion of phenylephrine (table, B).

Normocapnic ICBF was essentially constant over the MAP range of 60–110 mm Hg, with 10% decrease at 50 mm Hg. Thus the increase in $CO_2R$ with low MAP was a result of a higher absolute level of ICBF with hypercapnia.

The relation of $CO_2R$ to MAP was unaffected by baroreceptor denervation (table, C).

To give a more direct indication of the magnitude of the change in $CO_2R$ with MAP, data from groups A, B and C were pooled and mean $CO_2R$ was calculated at four MAP intervals: 45–60, 61–75, 76–90 and 91–105 mm Hg. Mean $CO_2R$'s and standard errors (SE) for these intervals were 17(1.7), 15(1.6), 13(1.8) and 11(1.7), respectively.

*Discussion.* Conflicting observations on relation of $CO_2R$ to MAP have been reported. In dogs, for instance, both a direct correlation of $CO_2R$ with MAP[7] and absence of such dependence[8] have been observed. In rabbits, on the other hand, a pressure dependence of $CO_2R$ has been described, but only for low MAP levels[9]. Since anesthetics are known to affect $CO_2R$[3] this divergence among reported findings may well be related to the effects of the anesthetics used (barbiturates, urethane), and the difficulty in controlling their effective levels when they are given i.v. For this reason, we used inhalation anesthesia where the anesthetic level can be finely adjusted and maintained constant.

The present results confirm our preliminary observations[3] that $CO_2R$ is inversely dependent on MAP. Moreover, this effect is independent of whether the MAP is increased pharmacologically or mechanically, and it apparently does not involve the baroreceptor reflex, since denervation of the arterial baroreceptors did not affect the correlation of $CO_2R$ and MAP. It is most likely that the alterations in $CO_2R$ resulted from changes in myogenic tone of the cerebral vessels. Thus, high MAP, by increasing the stretch on the vessel walls, might enhance the vascular tone and decrease the amount of vasodilatation produced by $CO_2$, while low MAP would have the opposite effect. An additional consideration is that hemodynamic changes accompanying the induced alterations in MAP may also have affected the apparent $CO_2R$ through modification of the peak arterial $PCO_2$ during the $CO_2$ test, or through a change in the effective alveolar (and plasma) concentration of the inhaled anesthetic.

1 This work was supported by grants from NIH (HL 17903) and American Heart Association – Greater Los Angeles Affiliate (437IG).
2 To whom requests for reprints should be sent.
3 Scremin, O.U., Rubinstein, E.H., and Sonnenschein, R.R., Stroke *9* (1978) 160.
4 Debley, V.G., J. appl. Physiol. *31* (1971) 138.
5 Scremin, O.U., Rubinstein, E.H., and Sonnenschein, R.R., J. cereb. Blood Flow Metab. *2* (1982) 55.
6 Winer, B.F., Statistical Principles in Experimental Design. McGraw-Hill Book Co., New York 1962.
7 Harper, A.M., and Glass, H.I., J. Neurol. Neurosurg. Psychiat. *28* (1965) 449.
8 Häggendal, E., and Johansson, B., Acta physiol. scand. *66* suppl. 258 (1965) 27.
9 Tuor, U.I., and Farrar, J.K., J. cereb. Blood Flow Metab. *1* suppl. 1 (1981) 184.

0014-4754/85/040467-02$1.50 + 0.20/0


## A somatotopic organization of leg afferents in the spider *Cupiennius salei* Keys. (Araneae, Ctenidae)

A. Brüssel and W. Gnatzy[1,2]

*Zoologisches Institut der J.W. Goethe-Universität, Gruppe Sinnesphysiologie, Siesmayerstrasse 70, D-6000 Frankfurt am Main (Federal Republic of Germany), 12 June 1984*

*Summary.* Axonal anterograde degeneration after ablation of different leg segments of the spider *Cupiennius salei* was traced using LM- and EM-methods. The pattern of degeneration seen in cross sections of the leg nerves close to their entry into the subesophageal ganglion shows a somatotopic organization of afferents within the leg nerves coming from different leg segments. All afferents run through the ventral part of the nerve.
*Key words.* Spider *Cupiennius salei;* leg segments; axonal anterograde degeneration; somatotopic organization; leg afferents.

In a nervous system, the arrangement of axons within peripheral nerves and the patterns of axon distribution which may exist, i.e. a somatotopic organization, are of interest for the interpretation of developmental and regeneration processes. Moreover, electrophysiological studies of the activity of specific receptors and investigations of the central projections require an exact knowledge of the courses of afferents within the ascending nerves.

In arthropods only a few reports are available concerning such somatotopic organization; all of them deal with insects[3]. We have studied this problem in a spider (Arachnoidea, Araneae). Using Wallerian anterograde degeneration we examined the arrangement of afferents within the leg nerves coming from different leg segments. Information about projections of leg afferents is essential for current studies of leg reflexes in *Cupiennius*[4].

*Materials and methods.* Adult females of the spider *Cupiennius salei* Keys. (Ctenidae) were used in all experiments. The main leg nerve in the 2nd and 4th walking legs of nine animals was cut into different leg segments under $CO_2$-anesthesia (see fig. 1 for the exact location of these sections). The operated as well as five control animals were then kept at room temperature for 33 h, 3, 4, 5, 6, 8 and 20 days, respectively. After subsequent re-anesthesia the subesophageal ganglion together with the stumps of the leg nerves were removed. The specimens were then prefixed in a buffered mixture of formaldehyde and glutaraldehyde, and postfixed in buffered osmiumtetroxide (see Gnatzy[5] for a detailed description of the method). The fixed specimens were embedded in Araldite. Cross sections of the leg nerves were made 2 mm from the subesophageal ganglion (see arrow in fig. 1). Sections 1 µm thick were stained with methylene blue for light microscopical examination and sections 80 nm thick were stained with lead citrate for electron microscopical study. The cross sections were traced with a semiautomatic image analyzer (Kontron MOP II) to determine their area.

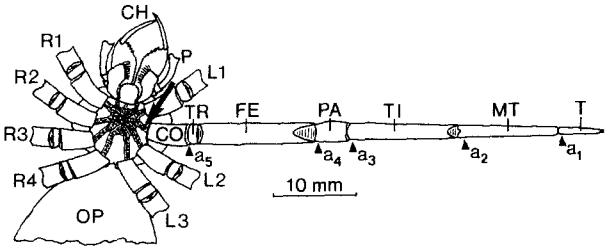


Figure 1. Schematized ventral view of *Cupiennius salei*. The sternum has been removed to show the location in which the nerve cross sections were taken for microscopic examination (long arrow). The four points ($a_1$–$a_4$) where the leg nerve was cut and the level of autonomy ($a_5$) are indicated by arrow heads. FE, femur; CH, chelicere; CO, coxa; L, left leg; MT, metatarsus; OP, opisthosoma; P, palpus; PA, patella; R, right leg; T, tarsus; TI, tibia; TR, trochanter.

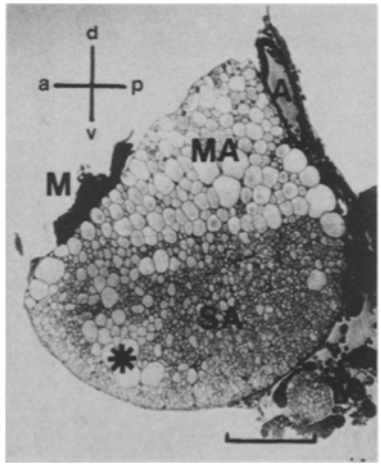


Figure 2. Cross section of the leg nerve (4th left leg, intact animal) showing the normal pattern of axon distribution. The orientation is the same in figure 4. a, anterior; d, dorsal; p, posterior; v, ventral; A, leg artery; M, muscle fibers; MA, motor axons; SA, sensory axons; *, large axons of the ventral part. Scale: 200 µm.

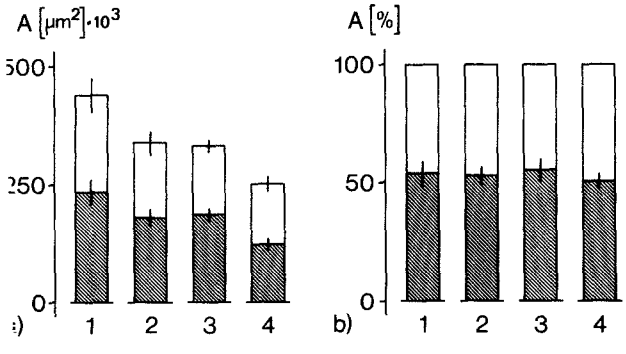


Figure 3. Cross-sectional areas of the four leg nerves (1–4). *a* Absolute values divided into motor (white) and sensory (hatched) axons, *b* percentage ratio of these values (n = 5).

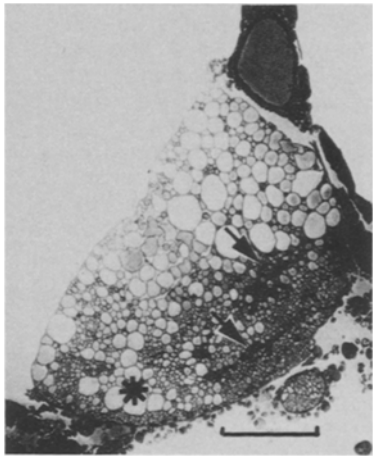


Figure 4. Cross section of the 4th right leg nerve showing the areas of degeneration (arrows) 4 days after amputation of the metatarsus (*, large axons of the ventral part). Scale: 200 µm.

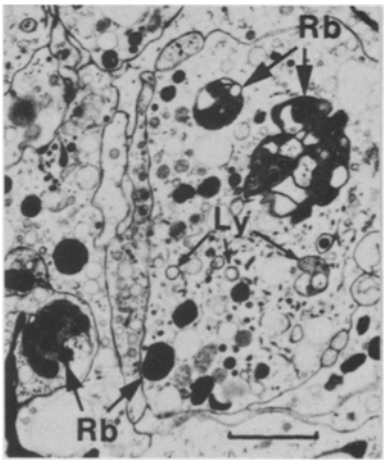


Figure 5. Degenerating sensory axons 8 days after dissection. Within the degenerating fibers there are lysosomes (Ly) and residual bodies (Rb). Scale: 5 µm.

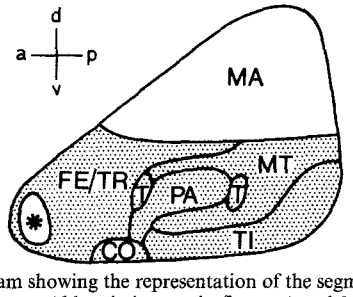


Figure 6. Diagram showing the representation of the segment's afferents within the leg nerve. Abbreviations as in figures 1 and 2.

*Results and discussion.* As in theraphosids[6] the three main leg nerves running through the leg of *Cupiennius salei* join in the coxa. In cross sections 2 mm from the CNS, this large nerve shows a bean-like shape (fig. 2). In contrast to insects, in which small and large fibers are distributed across the nerve's area[3,7,8], in *Cupiennius* there is a characteristic pattern of axon distribution: the dorsal portion of the leg nerve contains large axons ca 10–60 µm in diameter; the ventral part is filled up with small axons from 1 to 10 µm in diameter. Ventrally at the anterior edge are some large axons ca 20–50 µm in diameter (fig. 2). The cross-sectional area of the leg nerve decreases from the 1st to the 4th leg by about 40% (fig. 3a). This may indicate that a smaller number of axons run through the posterior legs. From axon counts in the tarsi of legs of the web spider *Zygiella x-notata* it is known that the 1st and 2nd legs contain up to 1500 sensory fibers; in the 3rd and 4th legs this number is considerable lower (600–800)[9].

The ratio between the area filled by large axons and that of the entire nerve is, however, similar for all legs (fig. 3b). As in insects, amputation of specific segments always results in degeneration of distinct regions within the nerve's cross section (fig. 4). Ablation of proximal segments causes degeneration of larger areas. These degenerations always occur in the ventral part of the nerve. Since in arthropods the sensory nerve cell bodies are located peripherally, only the sensory nerve fibers degenerate after amputation of peripheral leg segments. Therefore, one can distinguish a dorsal part with motor axons from a ventral part with sensory axons (compare fig. 2 with fig. 4). Figure 6 shows the representation of the afferents from the various segments within this ventral part of the leg nerve. A prominent feature is that all segments exept the tarsus are represented in a single distinct area: The metatarsus and the tibia in the posterior pole, the patella in the middle, the femur and trochanter in the anterior pole. The afferents of the coxa are located in a small area at the ventral margin of the nerve. The tarsus, however, is represented in two arrays in the middle next to the afferents of the patella.

The areas of the femur and the trochanter were determined together from autotomized legs (point $a_5$ in fig. 1). The coxa afferents were identified as the ones which remained intact after autotomy.

In general the degeneration process in the spider is similar to that in insects[3,7] as far as morphological symptoms are concerned. Initially the axoplasm darkens, then it clumps together and lysosomes and residual bodies appear (fig. 5). The glial sheath thickens and glial cells branch out. The fibers then lose their round shape and flatten. Finally the fibers collapse and the glial cells grow into the empty space. Differences exist in the time course of degeneration: In insects, 1 day after operation several axons have collapsed, and all fibers have collapsed after 6 days[3]. In *Cupiennius,* however, the degeneration process is much slower; axoplasmatic darkening does not appear earlier than 24 h after sectioning, collapse of some fibers happens only after 6 days, and all axons collapse only after 20 days post operation.

1 Acknowledgment. We thank Dr E.A. Seyfarth for helpful discussions. Parts of the study were supported by the Deutsche Forschungsgemeinschaft (W.G., SFB45/A1).
2 To whom all correspondence should be addressed.
3 Zill, S.N., Underwood, M.A., Rowley III, J.C., and Moran, D.T., Brain Res. *198* (1980) 253.
4 Seyfarth, E.A., J. comp. Physiol. *125* (1978) 45.
5 Gnatzy, W., Cell Tissue Res. *187* (1978) 1.
6 Rathmayer, W., Verh. dt. Zool. Ges. Jena (1966) 505.
7 Hess, A., Q. J. microsc. Sci. *99* (1958) 333.
8 Stocker, R.F., J. Morph. *160* (1979) 209.
9 Foelix, R.F., Müller-Vorholt, G., and Jung, H., Bull. Br. arachnol. Soc. *5* (1980) 20.

0014-4754/85/040468-03$1.50 + 0.20/0


## Chitin synthetase activity and inhibition in different insect microsomal preparations

E. Cohen

*Department of Entomology, Faculty of Agriculture, The Hebrew University, Rehovot 76-100 (Israel), 26 March 1984*

*Summary.* To facilitate massive screening and for structure-activity relationship studies of chitin synthesis inhibitors, methods to obtain the chitin synthetase (CS) containing microsomal fraction from the postmitochondrial supernatant were examined. Compared with fractionation by differential centrifugation, the $CaCl_2$ precipitate yielded the most active CS preparation. Acidification (pH 5.6) and polyethylene glycol 8000 (5%) treatments resulted in relatively low CS activity. Inhibitory effects were detected with polyoxin-D and 1-geranyl-2-methyl benzimidazole, a novel CS inhibitor, but not with benzoylphenyl ureas.
*Key words.* Chitin synthetase; microsomal fraction, insect; chitin synthesis inhibitors; flour beetle; *Tribolium castaneum.*

Chitin is an amino sugar biopolymer which serves as an essential structural component in insect cuticles[1,2] and in fungal cell walls[3]. Chitin has been considered as an attractive target for the action of selective pesticides since any interference with its normal pathway and timing of synthesis is detrimental. Recently several benzoylphenyl urea insecticides which act by blocking insect chitin synthesis have been developed. Based on the original discovery that DU-19111, a combination between dichlobenil and diuron, is insecticidal[4,5], several highly effective benzoylphenyl urea insecticides were prepared[6–8]. It has been established that these insecticides inhibit in vivo insect chitin synthesis[5,6]. However, chitin formation in fungi was insensitive to benzoylphenyl urea compounds[9,10]. Evidence from studies involving whole organisms and organ cultures suggests that chitin biosynthesis inhibition occurs at the polymerization step[6,9]. The precise biochemical lesion could be clarified by insect cell-free preparations capable of chitin polymerization. Such preparations have been recently obtained from *Tribolium castaneum* gut[11], integuments of *Trichoplusia ni* and *Hyalophora cecropia*[12] and from *Stomoxys calcitrans* whole pupae[13]. It appears that the insecticidal benzoylphenyl ureas do not affect directly the insect chitin synthetase (CS) (EC. 2.4.1.16)[10,13] and their action involves other possible mechanisms[14].

The *Tribolium* CS assay[11] is simple, reproducible and reliable. It can be useful for massive screening and evaluation of compounds acting as chitin synthetase inhibitors. For this assay, the microsomal fraction as the enzyme source is routinely prepared by differential centrifugation. In the present communication alternative methods in which the high-speed centrifugation step is avoided are explored. These methods are based